Proceedings of the 2006 American Control Conference
Minneapolis, Minnesota, USA, June 14-16, 2006

What Is the Ensemble Kalman Filter and How Well Does it Work?

S. Gillijns, O. Barrero Mendoza, J. Chandrasekar, B. L. R. De Moor, D. S. Bernstein, and A. Ridley

I. Introduction

While the classical Kalman filter provides a complete and rigorous solution for state estimation of linear systems under Gaussian noise, the estimation problem for nonlinear systems remains a problem of intense interest. Although rigorous solutions to the nonlinear problem have been studied, these results are either too narrow in applicability [2, 3] or are computationally expensive [4]. Consequently, a wide range of suboptimal methods have been examined for practical applications. The estimation problem is complicated by the fact that the distribution of the state is not completely characterized by the second moment, as is the case with linear systems. In particular, the probability density of the state evolves according to the Fokker-Planck partial differential equation [5].

The extended Kalman filter (XKF) [6] proceeds by adopting the formulae of the classical Kalman filter with the Jacobian of the dynamics matrix (in both continuous time and discrete time) playing the role of the linear dynamics matrix. This approach thus mimics the classical Kalman filter by propagating a matrix (the *surrogate covariance*) that is analogous to the error covariance in the linear case. Although XKF estimation is effective in many practical cases, the method fails to account for the fully nonlinear dynamics in propagating the error covariance, which, in turn, fails to represent the error probability density.

To avoid the use of the Jacobian, which may not exist for nonsmooth dynamics, the *state-dependent Riccati equation* (SDRE) approach retains the fully nonlinear dynamics by viewing the nonlinear plant dynamics as "frozen" linear dynamics [7, 8]. This approach requires a choice of frozen-linear dynamics, which are not unique. In addition, this method, like XKF estimation, propagates a surrogate error covariance.

In the present paper we consider yet another approach to nonlinear state estimation known as the *ensemble Kalman filter* (EnKF). While EnKF estimation has not been studied outside of specialized applications, its importance to specific problems is worthy of note. In particular, EnKF estimation is widely used in weather forecasting, where the models are of extremely high order and nonlinear, the initial states are highly uncertain, and a large number of measurements are available. There exist few textbook discussions of EnKF estimation. A brief overview of the technique is given in [9] and [10] . In the weather prediction literature, there exist a large number of papers that make use of the EnKF [11, 12].

The EnKF belongs to a broader category of filters known as *particle filters* [13, 14]. Unlike XKF estimation and SDRE estimation, particle filters use neither the Jacobian of the dynamics nor frozen linear dynamics. The starting point for particle filters is choosing a set of sample points, that is, an ensemble of state estimates, that captures the initial probability distribution of the state. These sample points are then propagated through the true nonlinear system and the probability density function of the actual state is approximated by the ensemble of the estimates.

In the case of the unscented Kalman filter [15] and the central difference Kalman filter [16], the sample points are chosen deterministically. In fact, the number of sample points required is of the same order as the dimension of the system. On the other hand, the number of ensembles required in the EnKF is heuristic. While one would expect that a large ensemble would be needed to obtain useful estimates, the literature on EnKF suggests that an ensemble of size 50 to 100 is often adequate for systems with thousands of states. The accuracy of the state estimates as a function of ensemble size is thus an important research question.

The present paper has three main goals. First, we summarize the steps of the EnKF estimation. Next, we apply the EnKF to a collection of three numerical examples to obtain insight into its effectiveness. In particular, we consider one linear example and two nonlinear examples, of both low order and high order. Our goal is to determine the tradeoff between ensemble size and estimation accuracy. Finally, using the results of these numerical studies, we speculate on those features that contribute to the performance of the EnKF in applications. Our hope is that this study will motivate future analytical investigations to better understand the effectiveness of EnKF in high-order, nonlinear applications.

II. The Extended Kalman Filter

Consider a discrete-time nonlinear system with dynamics

$$x_{k+1} = f(x_k, u_k) + w_k \tag{2.1}$$

and measurements

$$y_k = h(x_k) + v_k, \tag{2.2}$$

where $x_k, w_k \in \mathbb{R}^n$, $u_k \in \mathbb{R}^m$, y_k, and $v_k \in \mathbb{R}^p$. We assume that w_k and v_k are stationary zero-mean white noise processes with covariance matrices Q_k and R_k, respectively. Furthermore, we assume that x_0, w_k and v_k are uncorrelated.

This research was supported by the National Science Foundation Information Technology Research initiative, through Grant ATM-0325332 to the University of Michigan, Ann Arbor, USA .

S. Gillijns, O. Barrero Mendoza, and B.L.R. De Moor are with the Katholieke Universiteit Leuven, Belgium, bart.demoor@esat.kuleuven.ac.be

J. Chandrasekar, D. S. Bernstein, and A. Ridley are with The University of Michigan, Ann Arbor, MI 48109-2140, dsbaero@umich.edu.

1-4244-0210-7/06/$20.00 ©2006 IEEE

The objective is to obtain estimates x_k^{a} of the state x_k using measurements y_k so that $\mathrm{tr}\left(\mathcal{E}[e_k^{\mathrm{a}}(e_k^{\mathrm{a}})^{\mathrm{T}}]\right)$ is minimized, where $e_k^{\mathrm{a}} \in \mathbb{R}^n$ is defined by

$$e_k^{\mathrm{a}} \triangleq x_k - x_k^{\mathrm{a}}. \tag{2.3}$$

When the dynamics and measurement in (2.1) and (2.2) are linear, that is,

$$\begin{aligned} f(x_k, u_k) &= A_k x_k + B_k u_k, \\ h(x_k) &= C_k x_k, \end{aligned} \tag{2.4}$$

the Kalman filter provides optimal estimates x_k^{a} of the state x_k. Define the analysis state error covariance $P_k^{\mathrm{a}} \in \mathbb{R}^{n\times n}$ by $P_k^{\mathrm{a}} \triangleq \mathcal{E}\left[e_k^{\mathrm{a}}(e_k^{\mathrm{a}})^{\mathrm{T}}\right]$. The Kalman filter equations [1] are expressed in two steps, the analysis step, where information from the measurements is used, and the forecast step, where information about the plant is used. These steps are expressed as the analysis step:

$$K_k = P_{\mathrm{xy}_k}^{\mathrm{f}} \left(P_{\mathrm{yy}_k}^{\mathrm{f}}\right)^{-1}, \tag{2.5}$$

$$P_k^{\mathrm{a}} = (I - K_k C_k)\, P_k^{\mathrm{f}}, \tag{2.6}$$

$$x_k^{\mathrm{a}} = x_k^{\mathrm{f}} + K_k\left(y_k - C_k x_k^{\mathrm{f}}\right), \quad \text{(data update)} \tag{2.7}$$

and the forecast step:

$$x_{k+1}^{\mathrm{f}} = A_k x_k^{\mathrm{a}} + B_k u_k, \quad \text{(physics update)} \tag{2.8}$$

$$P_{k+1}^{\mathrm{f}} = A_k P_k^{\mathrm{a}} A_k^{\mathrm{T}} + Q_k, \tag{2.9}$$

where the forecast state error covariance $P_k^{\mathrm{f}} \in \mathbb{R}^{n\times n}$ is defined by $P_k^{\mathrm{f}} \triangleq \mathcal{E}\left[e_k^{\mathrm{f}}(e_k^{\mathrm{f}})^{\mathrm{T}}\right]$, and

$$\begin{aligned} P_{\mathrm{xy}_k}^{\mathrm{f}} &\triangleq \mathcal{E}\left[e_k^{\mathrm{f}}(y_k - y_k^{\mathrm{f}})^{\mathrm{T}}\right] = P_k^{\mathrm{f}} C_k^{\mathrm{T}}, \\ P_{\mathrm{yy}_k}^{\mathrm{f}} &\triangleq \mathcal{E}\left[(y_k - y_k^{\mathrm{f}})(y_k - y_k^{\mathrm{f}})^{\mathrm{T}}\right] = C_k P_k^{\mathrm{f}} C_k^{\mathrm{T}} + R_k, \end{aligned} \tag{2.10}$$

where $y_k^{\mathrm{f}} \triangleq C x_k^{\mathrm{f}}$, $e_k^{\mathrm{f}} \triangleq x_k - x_k^{\mathrm{f}}$.

However, when the dynamics in (2.1) are nonlinear, the discrete-time Riccati update equation (2.9) cannot be used to propagate the forecast state error covariance P_k^{f}. Propagating the state error covariance of a nonlinear system is generally difficult [3]. Hence, we consider approximate techniques for state estimation of nonlinear systems. One of the most widely used techniques for state estimation of nonlinear systems is the extended Kalman filter, where in the forecast step,

$$\begin{aligned} x_{k+1}^{\mathrm{f}} &= f(x_k^{\mathrm{a}}, u_k), \ \text{(physics update)} \\ P_{k+1}^{\mathrm{f}} &= A_k P_k^{\mathrm{a}} A_k^{\mathrm{T}} + Q_k, \end{aligned} \tag{2.11}$$

and in the data assimilation step,

$$\begin{aligned} x_k^{\mathrm{a}} &= x_k^{\mathrm{f}} + K_k(y_k - h(x_k^{\mathrm{f}})), \\ K_k &= P_k^{\mathrm{f}} C_k^{\mathrm{T}} (C_k P_k^{\mathrm{f}} C_k^{\mathrm{T}} + R_k)^{-1}, \\ P_k^{\mathrm{a}} &= P_k^{\mathrm{f}} - P_k^{\mathrm{f}} C_k^{\mathrm{T}} (C_k P_k^{\mathrm{f}} C_k^{\mathrm{T}} + R_k)^{-1} C_k P_k^{\mathrm{f}}, \end{aligned} \tag{2.12}$$

where the Jacobians $A_k \in \mathbb{R}^{n\times n}$ and $C_k \in \mathbb{R}^{p\times n}$ of $f(x,u)$ and $h(x)$, respectively, are defined by

$$A_k \triangleq \left.\frac{\partial f(x,u)}{\partial x}\right|_{x=x_k^{\mathrm{a}}}, \quad C_k \triangleq \left.\frac{\partial h(x)}{\partial x}\right|_{x=x_k^{\mathrm{a}}}. \tag{2.13}$$

III. The Ensemble Kalman filter

The ensemble Kalman filter (EnKF) is a suboptimal estimator, where the error statistics are predicted by using a Monte Carlo or ensemble integration to solve the Fokker-Planck equation. The Ensemble Kalman Filtering method is presented in three stages.

First, to represent the error statistics in the forecast step, we assume that at time k, we have an ensemble of q forecasted state estimates with random sample errors. We denote this ensemble as $X_k^{\mathrm{f}} \in \mathbb{R}^{n\times q}$, where

$$X_k^{\mathrm{f}} \triangleq (x_k^{\mathrm{f}_1}, \ldots, x_k^{\mathrm{f}_q}), \tag{3.1}$$

and the superscript f_i refers to the i-th forecast ensemble member. Then, the ensemble mean $\overline{x}_k^{\mathrm{f}} \in \mathbb{R}^n$ is defined by

$$\overline{x}_k^{\mathrm{f}} \triangleq \frac{1}{q}\sum_{i=1}^{q} x_k^{\mathrm{f}_i}.$$

Since the true state x_k is not known, we approximate (2.10) by using the ensemble members. We define the ensemble error matrix $E_k^{\mathrm{f}} \in \mathbb{R}^{n\times q}$ around the ensemble mean by

$$E_k^{\mathrm{f}} \triangleq \begin{bmatrix} x_k^{\mathrm{f}_1} - \overline{x}_k^{\mathrm{f}} & \cdots & x_k^{\mathrm{f}_q} - \overline{x}_k^{\mathrm{f}} \end{bmatrix} \tag{3.2}$$

and the ensemble of output error $E_{\mathrm{y}_k}^{\mathrm{a}} \in \mathbb{R}^{p\times q}$ by

$$E_{\mathrm{y}_k}^{\mathrm{a}} \triangleq \begin{bmatrix} y_k^{\mathrm{f}_1} - \overline{y}_k^{\mathrm{f}} & \cdots & y_k^{\mathrm{f}_q} - \overline{y}_k^{\mathrm{f}} \end{bmatrix}. \tag{3.3}$$

We then approximate P_k^{f} by $\hat{P}_k^{\mathrm{f}}$, $P_{\mathrm{xy}_k}^{\mathrm{f}}$ by $\hat{P}_{\mathrm{xy}_k}^{\mathrm{f}}$, and $P_{\mathrm{yy}_k}^{\mathrm{f}}$ by $\hat{P}_{\mathrm{yy}_k}^{\mathrm{f}}$, respectively, where

$$\begin{aligned} \hat{P}_k^{\mathrm{f}} &\triangleq \frac{1}{q-1} E_k^{\mathrm{f}} (E_k^{\mathrm{f}})^{\mathrm{T}}, \\ \hat{P}_{\mathrm{xy}_k}^{\mathrm{f}} &\triangleq \frac{1}{q-1} E_k^{\mathrm{f}} (E_{\mathrm{y}_k}^{\mathrm{f}})^{\mathrm{T}}, \ \hat{P}_{\mathrm{yy}_k}^{\mathrm{f}} \triangleq \frac{1}{q-1} E_{\mathrm{y}_k}^{\mathrm{f}} (E_{\mathrm{y}_k}^{\mathrm{f}})^{\mathrm{T}} \end{aligned} \tag{3.4}$$

Thus, we interpret the forecast ensemble mean as the best forecast estimate of the state, and the spread of the ensemble members around the mean as the error between the best estimate and the actual state.

The second step is the analysis step: To obtain the analysis estimates of the state, the EnKF performs an ensemble of parallel data assimilation cycles, where for $i = 1, \ldots, q$

$$x_k^{\mathrm{a}_i} = x_k^{\mathrm{f}_i} + \hat{K}_k\big(y_k^i - h(x_k^{\mathrm{f}_i})\big). \tag{3.5}$$

The *perturbed observations* y_k^i are given by

$$y_k^i = y_k + v_k^i, \tag{3.6}$$

where v_k^i is a zero-mean random variable with a normal distribution and covariance R_k. The sample error covariance matrix computed from the v_k^i converges to R_k as $q \to \infty$. We approximate the analysis error covariance P_k^{a} by $\hat{P}_k^{\mathrm{a}}$, where

$$\hat{P}_k^{\mathrm{a}} \triangleq \frac{1}{q-1} E_k^{\mathrm{a}} E_k^{\mathrm{a}\mathrm{T}},$$

and E_k^{a} is defined by (3.2) with $x_k^{\mathrm{f}_i}$ replaced by $x_k^{\mathrm{a}_i}$ and $\overline{x}_k^{\mathrm{f}}$ replaced by the mean of the analysis estimate ensemble members. We use the classical Kalman filter gain expression and the approximations of the error covariances to determine the filter gain $\hat{K}_k$ by

$$\hat{K}_k = \hat{P}_{\mathrm{xy}_k}^{\mathrm{f}} (\hat{P}_{\mathrm{yy}_k}^{\mathrm{f}})^{-1}. \tag{3.7}$$

The last step is the prediction of error statistics in the forecast step:

$$x_{k+1}^{\mathrm{f}_i} = f(x_k^{\mathrm{a}_i}, u_k) + w_k^i, \tag{3.8}$$

where the values w_k^i are sampled from a normal distribution with average zero and covariance Q_k. The sample error covariance matrix computed from the w_k^i converges to Q_k as $q \to \infty$. Finally, we summarize the analysis and forecast steps.

Analysis Step:

$$\begin{aligned} \hat{K}_k &= \hat{P}^{\mathrm{f}}_{\mathrm{xy}_k}(\hat{P}^{\mathrm{f}}_{\mathrm{yy}_k})^{-1}, \\ x_k^{\mathrm{a_i}} &= x_k^{\mathrm{f_i}} + \hat{K}_k\big(y_k + v_k^i - h(x_k^{\mathrm{f_i}})\big), \\ \overline{x}_k^{\mathrm{a}} &= 1/q \sum_{i=1}^{q} x_k^{\mathrm{a_i}}. \end{aligned} \tag{3.9}$$

Forecast Step:

$$\begin{aligned} x_{k+1}^{\mathrm{f_i}} &= f(x_k^{\mathrm{a_i}}, u_k) + w_k^i, \\ \overline{x}_{k+1}^{\mathrm{f}} &= 1/q \sum_{i=1}^{q} x_{k+1}^{\mathrm{f_i}}, \\ E_k^{\mathrm{f}} &= \begin{bmatrix} x_{k+1}^{\mathrm{f_1}} - \overline{x}_{k+1}^{\mathrm{f}} & \cdots & x_k^{\mathrm{f_q}} - \overline{x}_{k+1}^{\mathrm{f}} \end{bmatrix}, \\ E_{\mathrm{y}_k}^{\mathrm{a}} &= \begin{bmatrix} y_k^{\mathrm{f_1}} - \overline{y}_k^{\mathrm{f}} & \cdots & y_k^{\mathrm{f_q}} - \overline{y}_k^{\mathrm{f}} \end{bmatrix}, \\ \hat{P}^{\mathrm{f}}_{\mathrm{xy}_k} &= \frac{1}{q-1} E_k^{\mathrm{f}} (E_{\mathrm{y}_k}^{\mathrm{f}})^{\mathrm{T}}, \ \hat{P}^{\mathrm{f}}_{\mathrm{yy}_k} = \frac{1}{q-1} E_{\mathrm{y}_k}^{\mathrm{f}} (E_{\mathrm{y}_k}^{\mathrm{f}})^{\mathrm{T}}. \end{aligned} \tag{3.10}$$

Unlike the extended Kalman filter, the evaluation of the filter gain $\hat{K}_k$ in the EnKF does not involve an approximation of the nonlinearity $f(x,u)$ and $h(x)$. Hence, the computational burden of evaluating the Jacobians of $f(x,u)$ and $h(x)$ is absent in the EnKF. Furthermore, note that (2.11)-(2.12) in the XKF involves evaluation of $P_k^{\mathrm{f}} \in \mathbb{R}^{n\times n}$, which is an $\mathcal{O}(n^3)$ operation. However, in (3.9)-(3.10) of the EnKF, only $\hat{P}^{\mathrm{f}}_{\mathrm{xy}_k} \in \mathbb{R}^{n\times p}$ and $\hat{P}^{\mathrm{f}}_{\mathrm{yy}_k} \in \mathbb{R}^{p\times p}$, are evaluated, which is an $\mathcal{O}(pqn)$ operation. Hence, if $q \ll n$, then the computational burden of evaluating the approximate covariances in the EnKF is less than the computational burden of determining the approximate covariances in the XKF. However, (3.9) implies that q parallel copies of the model have to be simulated, and, when q is large, the computational burden of the forecast step in the EnKF is large. Alternatively, in the XKF, only one copy of the model is simulated to obtain the state estimates. Hence, if n is very large and $q \ll n$, then the EnKF is computationally less intensive than the XKF.

IV. Linear Example: Heat Conduction in a One-dimensional Bar

While the EnKF was developed with nonlinear estimation problems in mind, we start with a linear heat conduction example. The reason for this example is twofold. Firstly, our main objective, the determination of parameters that contribute to the tradeoff between ensemble size and estimation accuracy, will not be influenced by nonlinear effects. Secondly, we can calculate the optimal state estimates using the Kalman filter. A comparison between the EnKF and KF thus demonstrates the tradeoff between the number of ensemble members needed and accuracy in estimation.

Consider the heat conduction in a one-dimensional bar, governed by the equation

$$\frac{\partial T(x,t)}{\partial t} = \alpha \frac{\partial^2 T(x,t)}{\partial x^2} + u(x,t), \tag{4.1}$$

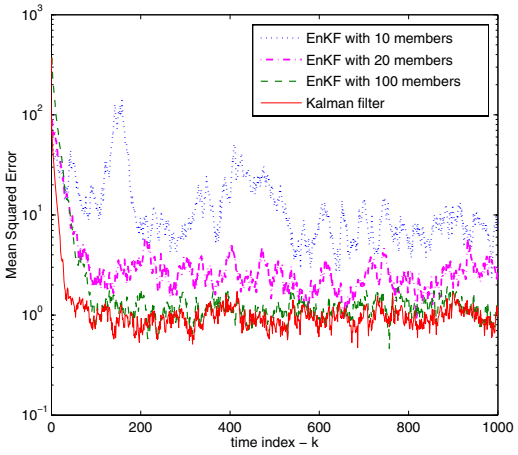

Fig. 1. Mean squared error between the estimates obtained from the EnKF estimator with 10, 20 and 100 ensemble members and the state of the truth model. The MSE of the KF estimates is also plotted for comparison.

where $T(x,t)$ is the temperature at position x and time t, $u(x,t)$ represents external heat sources acting on the bar, and α is the heat conduction coefficient. The initial and boundary conditions are $T(x,0) = T(0,t) = T(L,t) = 300\mathrm{K}$, where L is the length of the bar. Two sinusoidally varying heat sources are acting on the bar at positions $0.33L$ and $0.67L$, respectively. Using a central difference method, (4.1) is discretized over a spatial grid with $n = 100$ cells, resulting in the linear time invariant model

$$x_{k+1} = Ax_k + Bu_k + w_k, \tag{4.2}$$

where $A \in \mathbb{R}^{100\times 100}$ is tridiagonal, B is chosen such that the input $u_k \in \mathbb{R}^2$ affects cells 33 and 67, and w_k is assumed to be zero-mean white Gaussian process noise with covariance matrix $Q = 0.5I_n$.We assume that noisy measurements y_k of the temperature at cells $10, 20, \ldots, 90$ are available and v_k is zero-mean white Gaussian noise with covariance $R = 0.01I_9$.

We first simulate the truth model from an arbitrary initial condition x_0. A low number of ensemble members leads to sampling errors, which implies that the sample error covariance matrix computed from the w_k^i is different from the actual process noise covariance matrix Q, degrading the performance of the filter. The mean squared error (MSE) in the state estimates is shown in Figure 1 for the KF, the EnKF with 10, 20, and 100 ensemble members. As expected, the accuracy of the EnKF increases when the number of ensemble members grows. Figure 2 shows the evolution of the MSE as a function of the ensemble size. This is an illustration of the tradeoff between accuracy and number of ensemble members.

V. Nonlinear Example: Van der Pol Oscillator

Next, we compare the performance of the XKF estimator and the EnKF estimator on a low dimensional nonlinear example. A first-order Euler discretization of the equations

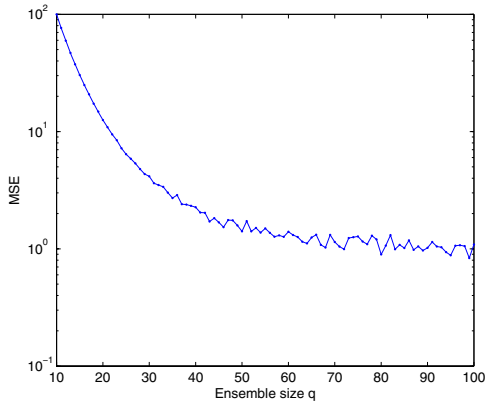

Fig. 2. MSE as a function of ensemble size. This is an illustration of the tradeoff between accuracy and the ensemble size.

of motion of the Van der Pol oscillator yields

$$x_{k+1} = f(x_k), \tag{5.1}$$

where $x_k = \begin{bmatrix} x_{1,k} & x_{2,k} \end{bmatrix}^{\mathrm{T}}$,

$$f(x_k) = \begin{bmatrix} x_{1,k} + h x_{2,k} \\ x_{2,k} + h\left(\alpha(1 - x_{1,k}^2)x_{2,k} - x_{1,k}\right) \end{bmatrix}, \tag{5.2}$$

and h is the step size. We assume that the Van der Pol oscillator is driven by w_k, that is,

$$x_{k+1} = f(x_k) + w_k, \tag{5.3}$$

where $w_k \in \mathbb{R}^2$ is zero-mean white Gaussian noise with covariance matrix $Q \in \mathbb{R}^{2\times 2}$. We assume that for all $k \geqslant 0$, measurements of either $x_{1,k}$ or $x_{2,k}$ are available so that

$$y_k = Cx_k + v_k, \tag{5.4}$$

where $v_k \in \mathbb{R}$ is zero mean white Gaussian noise with covariance $R > 0$ and C selects $x_{1,k}$ or $x_{2,k}$. The objective is to obtain estimates x_k^{a} of the state x_k using measurements y_k in an extended Kalman filter. Note that the XKF estimator requires the Jacobian of the function $f(x)$, whereas the EnKF estimator does not require the Jacobian. Let $\alpha = 1$ and the step size $h = 0.1$ so that the discrete-time system (5.1) is stable. Let the noise covariances of w_k and v_k be $Q = \mathrm{diag}(0.0262, 0.008)$ and $R = 0.003$, respectively. We first simulate the truth model (5.3) from an arbitrary initial condition $x_0 \in \mathbb{R}^2$. Next, we assume that $x_0^{\mathrm{f}} \neq x_0$ and use measurements y_k of $x_{2,k}$ so that $C = \begin{bmatrix} 0 & 1 \end{bmatrix}$, to obtain estimates x_k^{a} of x_k. The extended Kalman filter gain K_k is obtained using (2.5), (2.11)-(2.13) and the initial condition $P_0^{\mathrm{f}} = \mathrm{diag}(6.3e-4, 2.2e-4)$. The state estimates and the MSE in the state estimates of x_k obtained by using measurements of $x_{2,k}$ in the XKF are shown in Figures 3 and 4, respectively. The state estimates obtained from the EnKF when 5, 10, and 30 ensemble members are used, are also shown in Figure 3. The MSE in the state estimates obtained from the EnKF is shown in Figure 4. In this case the performance of the EnKF estimator with 5 ensembles is the same as the performance of the extended Kalman filter. However, as the ensemble size q increases, the performance

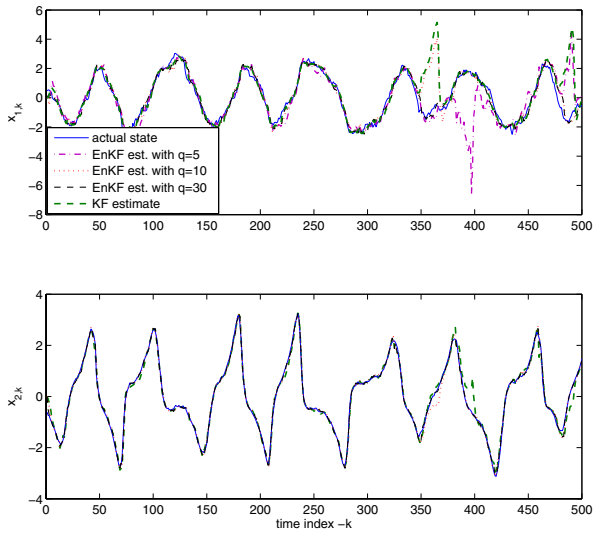

Fig. 3. State estimates x_k^{a} of the noise driven Van der Pol oscillator when measurements of $x_{2,k}$ are used in the EnKF estimator. The state estimates from the EnKF with $q = 5, 10$, and 30 ensembles is also plotted. The state estimates improve as more ensembles are used.

of the EnKF improves and the performance of the EnKF with 30 ensembles is better than the performance of the XKF.

VI. Nonlinear Example: One-dimensional Hydrodynamic Flow

We consider the flow of an inviscid, compressible fluid along a one-dimensional channel. The dynamics of hydrodynamic flow are governed by Euler's equations

$$\begin{aligned} \frac{\partial \varrho}{\partial t} &= -\frac{\partial}{\partial x}\varrho v, \\ \frac{d}{dt}\left(\frac{p}{\varrho^\gamma}\right) &= 0, \\ \varrho\frac{\partial v}{\partial t} &= -\varrho v\frac{\partial v}{\partial x} - \frac{\partial p}{\partial x}, \end{aligned} \tag{6.1}$$

where $\varrho \in \mathbb{R}$ is the density, $v \in \mathbb{R}$ is the velocity, $p \in \mathbb{R}$ is the pressure of the fluid, and $\gamma = \frac{5}{3}$ is the ratio of specific heat of the fluid. Due to the presence of coupled partial differential equations, it is generally difficult to obtain closed-form solutions of (6.1). However, a discrete-time model of hydrodynamic flow can be obtained by using a finite-volume based spatial and temporal discretization.

Assume that the channel consists of n identical cells. For all $i = 1, \ldots, n$, let $\varrho^{[i]}$, $v^{[i]}$, and $p^{[i]}$ be the density, velocity, and pressure in the ith cell. We use a second-order Rusanov scheme [17] to discretize (6.1) and obtain a discrete-time model that enables us to update the flow variables at the center of each cell. We assume that the flow variables at cells 1 and 2 are determined by the boundary conditions u_k so that

$$\begin{bmatrix} \varrho_k^{[1]} & m_k^{[1]} & \mathcal{E}_k^{[1]} & \varrho_k^{[2]} & m_k^{[2]} & \mathcal{E}_k^{[2]} \end{bmatrix}^{\mathrm{T}} = u_k. \tag{6.2}$$

Furthermore, we assume Neumann boundary conditions for

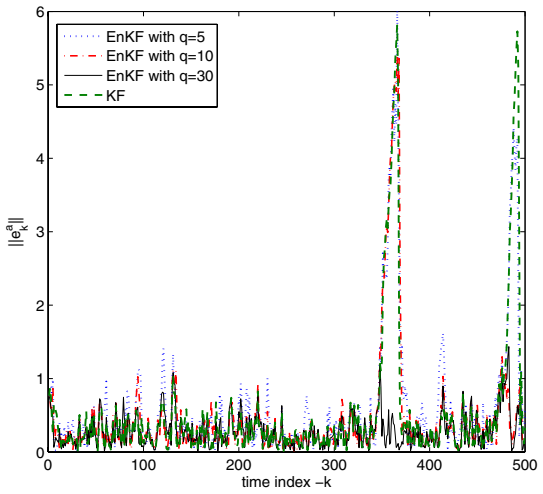

Fig. 4. Norm of the error $\|e_k\|$ between the state of the truth model x_k and its ensemble Kalman filter estimate x_k^{a} is shown. The error in the state estimates decreases as the number of ensembles increases and the performance of the EnKF estimator with $q = 30$ ensembles is better than the performance of the XKF estimator.

the cells with index $n-1$ and $n-2$ so that, for all $k \geqslant 0$,

$$\begin{bmatrix} \varrho_k^{[n]} \\ m_k^{[n]} \\ \mathcal{E}_k^{[n]} \end{bmatrix} = \begin{bmatrix} \varrho_k^{[n-1]} \\ m_k^{[n-1]} \\ \mathcal{E}_k^{[n-1]} \end{bmatrix} = \begin{bmatrix} \varrho_k^{[n-2]} \\ m_k^{[n-2]} \\ \mathcal{E}_k^{[n-2]} \end{bmatrix}, \tag{6.3}$$

where, for all $i = 1, \ldots, n$, the momentum $m^{[i]}$ and energy $\mathcal{E}^{[i]}$ in the ith cell are given by

$$m^{[i]} = \varrho^{[i]} v^{[i]}, \quad \mathcal{E}^{[i]} = \frac{1}{2}\varrho^{[i]}(v^{[i]})^2 + \frac{p^{[i]}}{\gamma - 1}. \tag{6.4}$$

Finally, define the state vector $x \in \mathbb{R}^{3(n-4)}$ by

$$x \triangleq \begin{bmatrix} \varrho^{[3]} & m^{[3]} & \mathcal{E}^{[3]} & \cdots \varrho^{[n-2]} & m^{[n-2]} & \mathcal{E}^{[n-2]} \end{bmatrix}^{\mathrm{T}}. \tag{6.5}$$

Using a second-order Rusanov scheme [17] yields a nonlinear discrete-time update model of the form

$$x_{k+1} = f(x_k, u_k). \tag{6.6}$$

Let $n = 40$ so that $x \in \mathbb{R}^{108}$. For all $k \geqslant 0$, let $u_k \in \mathbb{R}^3$ denote the boundary condition for the first two cells, so that

$$u_k = \begin{bmatrix} \varrho_k^{[1]} & m_k^{[1]} & \mathcal{E}_k^{[1]} \end{bmatrix}^{\mathrm{T}} = \begin{bmatrix} \varrho_k^{[2]} & m_k^{[2]} & \mathcal{E}_k^{[2]} \end{bmatrix}^{\mathrm{T}}. \tag{6.7}$$

For all $k \geqslant 0$, we choose $\varrho_k^{[1]} = \varrho_k^{[2]} = 1$, $v_k^{[1]} = v_k^{[2]} = 1 + 0.1\sin(0.5k)$, and $p_k^{[1]} = p_k^{[2]} = 1$. We assume that the truth model is given by

$$x_{k+1} = f(x_k, u_k) + w_k, \tag{6.8}$$

where $w_k \in \mathbb{R}^{3(n-4)}$ represents unmodeled drivers and is assumed to be zero-mean white Gaussian process noise with covariance matrix $Q \in \mathbb{R}^{3(n-4)\times 3(n-4)}$, where

$$Q = \mathrm{diag}(Q^{[3]}, Q^{[4]}, \ldots, Q^{[n-2]}) \tag{6.9}$$

and, for all $i = 3, \ldots, n-2$, $Q^{[i]} \in \mathbb{R}^{3\times 3}$ is defined by

$$Q^{[i]} = \begin{cases} \mathrm{diag}(0.001, 0.005, 0.01), & \text{if } i = 10, 30, \\ 0_{3\times 3}, & \text{else.} \end{cases} \tag{6.10}$$

It follows from (6.8)-(6.9) that the flow variables in only the 10th and 30th cell are directly affected by w_k. Next, assume that the measurement $y_k \in \mathbb{R}^6$ of density, momentum and energy at the 16th and 17th cells is given by

$$y_k = Cx_k + v_k, \tag{6.11}$$

where $C \in \mathbb{R}^{6\times 3(n-4)}$ and $v_k \in \mathbb{R}^6$ is zero-mean white Gaussian noise with covariance matrix $R = 0.001 I_{6\times 6}$. We simulate the truth model (6.8) from an arbitrary initial condition $x_0 \in \mathbb{R}^{3(n-4)}$ and obtain measurements y_k from (6.11). The objective is to estimate the density, momentum and energy at the cells where measurements of flow variables are unavailable using the XKF and the EnKF.

Note that the extended Kalman filter (2.11)-(2.13) requires the Jacobian of the nonlinear function $f(x, u)$. However, $f(x, u)$ in (6.6) is obtained using the second-order Rusanov scheme and contains the non-differentiable functions $\mathrm{abs}(\cdot)$ and $\max(\cdot, \cdot)$. Hence, A_k defined in (2.13) does not exist. Hence, let $\hat{f}(x, u)$ be an approximation of $f(x, u)$ in (6.8) obtained by replacing all non-differentiable functions in $f(x, u)$ with differentiable approximations. For example, the $\mathrm{abs}(x)$ function can be approximated by $\tanh(\alpha x)$, where $\alpha > 0$ is large. Next, define the Jacobian $\hat{A}_k$ of $\hat{f}(x, u)$ by (2.13) with $f(x, u)$ replaced by $\hat{f}(x, u)$. Although an analytical expression for $\hat{A}_k$ can be obtained, numerical techniques are typically used to obtain an approximate Jacobian. Due to the large dimension of the system, obtaining an analytical expression for $\hat{A}_k$ is tedious and hence, we use a numerical approximation $\tilde{A}_k$ of $\hat{A}_k$.

The estimates x_k^{f} from the extended Kalman filter are obtained from (2.11)-(2.13) with A_k replaced by $\tilde{A}_k$ and initial conditions

$$\begin{aligned} x_0^{\mathrm{f}} &= \begin{bmatrix} 1 & 1 & 1.5 & \cdots & 1 & 1 & 1.5 \end{bmatrix}^{\mathrm{T}}, \\ P_0^{\mathrm{f}} &= 0.001 I_{3(n-4)\times 3(n-4)}. \end{aligned} \tag{6.12}$$

The state estimates from the ensemble Kalman filter are obtained from (3.9)-(3.10). The ensemble size q is varied and, for all $i = 1, \ldots, q$, the initial ensemble members $x_0^{\mathrm{f}_i}$ are assumed to be random variables with mean x_0^{f} and covariance P_0^{f}. Figure 5 shows the MSE between the estimates x_k^{f} and state x_k when no data assimilation is performed and when measurements y_k are used in the extended Kalman filter. The error in the state estimates obtained using the ensemble Kalman filter with ensemble size $q = 25, 40, 60$, and 80 is shown in the same figure. It can be seen that the error in the estimate of the flow variables decreases as the ensemble size is increased from 25 to 60. However, the performance of the EnKF estimator with 60 ensemble members is the same as the performance of the EnKF with 80 ensemble members. Hence, further improvement in the performance cannot be achieved by increasing the ensemble member size q.

Figure 6 shows the density profile of the truth model at $t =$ 190s. The density profiles obtained by using the estimates of the extended Kalman filter and the ensemble Kalman filter are also plotted. As the ensemble size q is increased, the performance of the EnKF improves and as shown in Figure

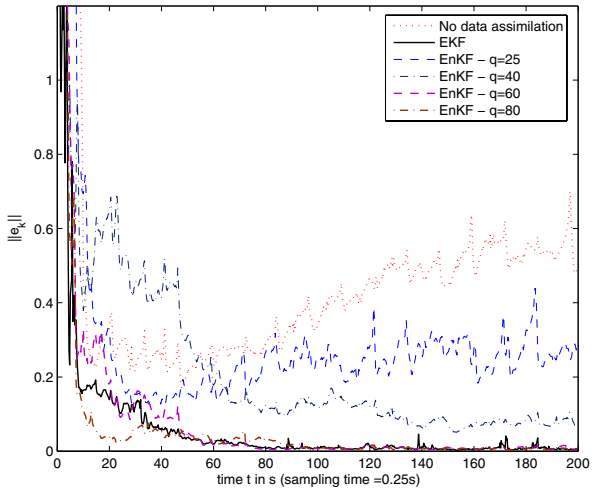

Fig. 5. Norm of the error $\|e_k\|$ between the state of the truth model x_k and its estimate x_k^{a}. The error in the state estimates when no data assimilation is performed is shown as a dashed line (–). The MSE in the state estimates obtained from the extended Kalman filter and the ensemble Kalman filter with $q = 25$, 40, 60, and 80 is also plotted.

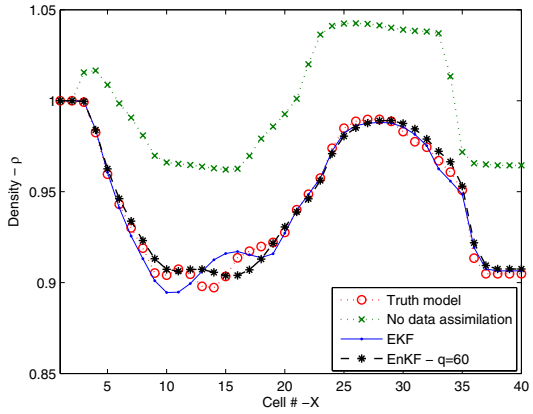

Fig. 6. Profile of the density ρ at $t = 190$s. The actual density profile and the density profile from the state estimates obtained using the extended Kalman filter and the ensemble Kalman filter are shown. The density profile when no data assimilation is performed is also shown in the figure for comparison.

7, the computational time required to calculate the estimates also increases. The time taken to simulate 200 s of flow in the truth model is also shown in Figure 7 for comparison. The simulations were performed using MATLAB 7.0 on a Pentium 4, 3.2 GHz processor. The huge computational time in the XKF is due to the huge matrix multiplication required to evaluate the covariance, and the numerical procedure used to obtain the Jacobian.

VII. Conclusion

In this paper we described the ensemble Kalman filter algorithm. This approach to nonlinear Kalman filtering is a Monte Carlo procedure, which has been widely used in weather forecasting applications. Our goal was to apply the ensemble Kalman filter to representative examples to quantify the tradeoff between estimation accuracy and ensemble size. For all of the linear and nonlinear examples that we considered, the ensemble Kalman filter worked successfully once a threshold ensemble size was reached. In future work we will investigate the factors that determine this threshold value.

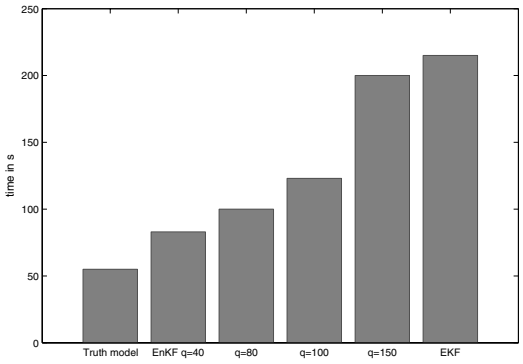

Fig. 7. Time required to simulate 200 s of hydrodynamics flow using the truth model. The time required to obtain the state estimates using the XKF and EnKF is shown.

References

[1] B. D. O. Anderson and J. B. Moore, *Optimal Filtering*, Prentice-Hall, 1979.

[2] V. E. Benes, "Exact Finite-Dimensional Filters For Certain Diffusions with Nonlinear Drift,"*Stochastics*, vol. 5, pp. 65-92, 1981.

[3] F. E. Daum, "Exact Finite Dimensional Nonlinear Filters," *IEEE Trans. Automatic Control*, vol. AC-31, no. 7, pp. 616-622, July 1986.

[4] A. J. Krener and A. Duarte, "A Hybrid Computational Approach to Nonlinear Estimation," *Proc. Conf. Dec. Contr.*, Kobe, Japan, pp. 1815-1819, December 2004.

[5] A. Jazwinski, *Stochastic Processes and Filtering Theory,* New York : Academic Press, 1970.

[6] A. Gelb, *Applied Optimal Estimation,* The M.I.T Press, 1974.

[7] J. Chandrasekar, A. Ridley, and D. S. Bernstein, "A SDRE-Based Asymptotic Observer for Nonlinear Discrete-Time Systems," *Proc. Amer. Contr. Conf.,* Portland, Oregon 2005, pp. 3630-3635.

[8] C. P. Mracek, J. R. Cloutier, and C. A. D'Souza, "A New Technique for Nonlinear Estimation," *Proc. IEEE Conf. Contr. App.,* 1996, pp. 338-343.

[9] R. Daley, *Atmospheric Data Analysis*, Cambridge University Press, 1991.

[10] E. Kalnay, *Atmospheric modeling, data assimilation and predictability,* Cambridge University Press, 2003.

[11] G. Evensen, "Advanced Data Assimilation for Strongly Nonlinear Dynamics," Monthly Weather Review, vol. 125, pp. 1342-1354, 1997.

[12] G. Evensen, "Sequential Data Assimilation for Nonlinear Dynamics: The Ensemble Kalman Filter," *In Ocean Forecasting: Conceptual basis and applications,* edited by N. Pinardi and J. D. Woods, Springer-Verlag Berlin Heidelberg, 2002.

[13] F. E. Daum and J. Huang, "The Curse of Dimensionality for Particle Filters," *Proc. IEEE Conf. Aero.*, vol. 4, pp. 1979-1993, 2003.

[14] J. H. Kotecha and P. M. Djuric, "'Gaussian particle filtering," *IEEE Trans. Sig. Proc.,* vol. 51, pp. 2592 - 2601, 2003.

[15] E. A. Wan and R. van der Merwe, "The Unscented Kalman Filter for Nonlinear Estimation," *Proc. The IEEE AS-SPCC Symposium,* 2000.

[16] K. Ito and K. Xiong, "Gaussian Filters for Nonlinear Filtering," *IEEE Trans. Auto. Cont.*, vol. 45, pp. 910927, 2000.

[17] C. Hirsch, *Numerical Computation of Internal and External Flows,* pp. 408-469, John Wiley and Sons, 1994.